



Contents lists available at ScienceDirect

Indian Pacing and Electrophysiology Journal

journal homepage: www.elsevier.com/locate/IPEJ

A case of successful radiofrequency catheter ablation for atrial tachycardia originating from the inferior vena cava using high-resolution mapping

Yusaku Fukumoto^a, Yuji Kamikawa^a, Tatsuya Koike^a, Masahiro Esato^{b,*}^a Department of Cardiology, Sendai Tokushukai Hospital, Sendai City, Japan^b Department of Cardiology, Heart Rhythm Section, Ogaki Tokushukai Hospital, Ogaki City, Japan

ARTICLE INFO

Article history:

Received 23 March 2022

Received in revised form

18 June 2022

Accepted 24 June 2022

Available online 28 June 2022

Keywords:

Catheter ablation

Atrial tachycardia

Three-dimensional high-resolution mapping

ABSTRACT

A 60-year-old man presented with sustained supraventricular tachycardia. Atrial tachycardia (AT), with the earliest atrial activation (EAA) occurring at the ostium of the coronary sinus, was reproducibly induced.

Three-dimensional electroanatomical mapping (3DEAM) using a 3.5-mm distal electrode tip linear catheter (Thermocool) and radiofrequency energy (RF) was performed at the fractionated atrial electrogram site. It preceded at 30 ms to the EAA but did not terminate AT. Further 3DEAM using a multi-electrode mapping catheter (Pentaray) demonstrated a centrifugal propagation pattern at the boundary zone between the right atrium and inferior vena cava. RF application here terminated AT, which then became non-inducible.

© 2022 Indian Heart Rhythm Society. Published by Elsevier B.V. This is an open access article under the CC BY-NC-ND license (<http://creativecommons.org/licenses/by-nc-nd/4.0/>).

1. Introduction

Three-dimensional electroanatomic mapping (3DEAM) systems have been developed to identify triggers or substrates of various complex tachyarrhythmias. Its introduction has greatly facilitated radiofrequency catheter ablation (RFCA) procedures. As 3DEAM uses point-by-point registration of the spatial distribution of cardiac functional characteristics (i.e., localized electrical potentials), detailed and accurate acquisition of the electrical potentials from the bipolar/unipolar electrode recordings is essential. We here present a case of atrial tachycardia (AT) originating from the inferior vena cava (IVC), which successfully identified and eliminated by RFCA using high-resolution mapping.

2. Case

A 60-year-old male was admitted to our institution due to persistent palpitation, the cause of which we were unable to confirm for several years. A 12-lead surface electrocardiogram

(ECG) documented supraventricular tachycardia (SVT) with a ventricular rate of 146 bpm. Additionally, a nonsustained ectopic atrial rhythm, in which the P wave morphology (PWM) was markedly different from the morphology of the sinus rhythm, was observed during hospitalization. The polarity of the P wave was negative in the inferior limb leads (II/III/aVF) and isoelectric-negative in V1 and V4-6 (Fig. 1). Several screening tests, such as echocardiography, enhanced coronary computed tomography, and laboratory data from blood samples, disclosed no evident abnormalities. Due to the frequent symptoms of SVT, an electrophysiological study (EP) followed by RFCA was performed after the patient's consent to treatment was obtained in writing.

Propofol was administered to alleviate the patient's discomfort during the procedure and pentazocine was used for pain relief if necessary. EP was enforced via three 5-Fr 4-pole and one 6-Fr 10-pole electrode catheters. The former were inserted through the right femoral vein and positioned in the high lateral right atrium (HRA), the His bundle electrogram recorded site (HBE), and the right ventricular apex (RVA), while the latter was inserted into the coronary sinus (CS) from the right jugular vein. SVT was reproducibly induced via single premature contraction or was spontaneously induced using isoproterenol infusion. However, no sustained SVT was induced during atrial rapid/programmed stimulation. The majority of the cycle length of induced SVT was 450 ms,

* Corresponding author. Department of Cardiology, Heart Rhythm Section, Ogaki Tokushukai Hospital, 6-85-1 Hayashi-machi, Ogaki City, Gifu, 503-0015, Japan.

E-mail address: rfca_erichann0045@yahoo.co.jp (M. Esato).

Peer review under responsibility of Indian Heart Rhythm Society.

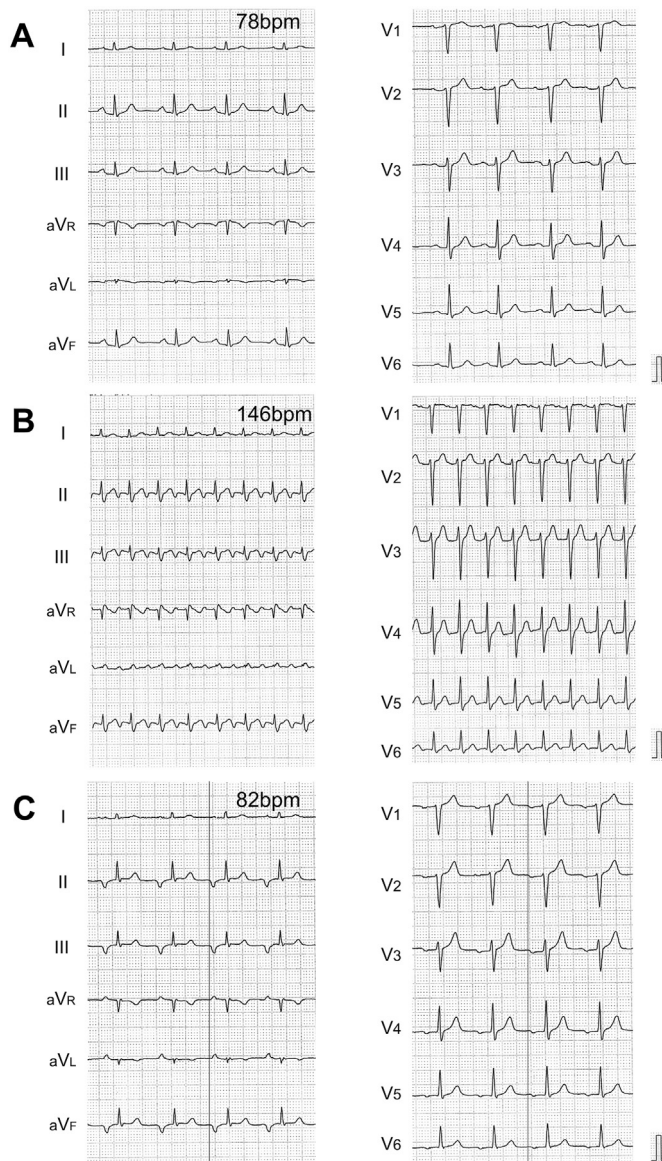


Fig. 1. A 12-lead surface electrocardiogram **A.** at rest, **B.** during supraventricular tachycardia, and **C.** during ectopic atrial rhythm. Black-color vertical lines in both limb and precordial leads are obtained just before the onset of the P wave. BPM, beats per minute.

while a cycle length of 650–700 ms, identical to that of ectopic atrial rhythm (documented from 12-lead ECG), with a gradual cycle length shortening during initiation, was also observed. The earliest atrial activation (EAA) during SVT was consistently observed from the electrodes positioned at the ostium of the CS (Fig. 2).

Regarding the differential diagnosis, tachycardia was diagnosed as AT according to the following electrophysiological characteristics: 1. Retrograde ventriculoatrial (VA) conduction was not observed during RVA stimulation, 2. A 1:1 VA synchronized relationship was noted during tachycardia, and 3. The ventricular activation was not linked to the atrial activation (termed as “no VA linking”), as demonstrated by atrial overdriving stimulation from different atrial sites [1]. Catheter mapping was therefore performed to detect the AT origin.

Initially, 3DEAM was performed using a conventional 3.5-mm distal electrode tip linear catheter (Thermocool SmartTouch®SF, Biosense Webster, Diamond Bar, CA, USA), adjacent to the ostium of

the CS, corresponding to the EAA site. Radiofrequency (RF) energy application (30 W, 12 mL/min. Flow from the irrigated tip) was attempted at the site where a fractionated potential preceded the P wave onset by 75 ms and the EAA site by 30 ms; however, this did not terminate AT. Therefore, additional 3DEAM was performed using a multielectrode mapping catheter (Pentaray® NAV ECO, Biosense Webster, Diamond Bar, CA, USA). The local activation map from the re-constructed 3DEAM demonstrated a centrifugal pattern radiating from the boundary zone between the right atrium (RA) and the IVC. The potential recorded from the EAA site obtained from the multielectrode catheter preceded the P wave onset by 105 ms, the QS pattern from the unipolar, and 0.27 mV from the bipolar electrode (Fig. 3). RF energy re-application after positioning the ablation catheter at that site immediately terminated AT, although no distinct potential was observed from the distal part of the bipolar electrode of the ablation catheter (Fig. 4). The patient did not complain of any type of arrhythmogenic recurrence over the following 6 months.

3. Discussion

The main findings in the present case were as follows: 1. The AT origin, diagnosed as a focal mechanism from 3DEAM, was from the ostium region of the IVC, which is not a well-known site for atrial tachyarrhythmogenesis, and 2. AT was successfully eliminated by detecting its precise origin using high-density mapping technology via a multielectrode catheter.

Regarding focal AT, several previous studies have retrospectively investigated the origin and characteristics of PWM from a 12-lead surface ECG by reviewing the successful RFCA site [2,3]. In this series, however, no detailed information was obtained, and no analyses were performed for focal AT arising from the IVC, as in the present case. Little is known about the arrhythmogenesis of the IVC, although other thoracic veins, such as the CS, pulmonary veins (PVs), and supra vena cava (SVC) are recognized as the major sources of atrial tachyarrhythmias [4–6]. Kholová et al. reported that although myocardial extensions were almost always found in both the SVC and IVC in human autopsied hearts, a frequent absence of an electrical connection between the IVC and RA myocardium would make the IVC electrically less active than the SVC [7]. This difference in electrical and mechanical activities between the IVC and the other thoracic veins mentioned above may explain the limited information regarding IVC arrhythmogenesis. The present case, together with other previous cases, such as the focal rapid discharges of atrial fibrillation instead of AT as in the present case, support the possibility that the IVC can be a focal source of atrial tachyarrhythmia [8,9].

Identifying the precise mechanism of AT; either reentry, triggered activity, or enhanced automaticity, is also of great importance. In the present case, AT was not induced in any type of atrial or ventricular stimulation favoring a non-reentrant mechanism. Although it is not entirely sufficient to exclude the mechanism of triggered activity, the electrophysiological characteristics, including spontaneously inducible with a gradual shortening of the tachycardia cycle length during AT initiation (i.e., warming up phenomenon), and all ATs with different tachycardia cycle lengths became noninducible by focal RF application, deserve the diagnosis as enhanced automaticity.

The origin of AT was successfully identified and eliminated using high-resolution mapping via a multielectrode catheter in the present case. Notably, no marked potential was observed from the distal tip of the bipolar electrode of the ablation catheter, positioned at the successful RFCA site. Anter et al. compared mapping resolution using either a conventional 3.5-mm electrode catheter (Thermocool ablation catheter) or by using a 1-mm multielectrode

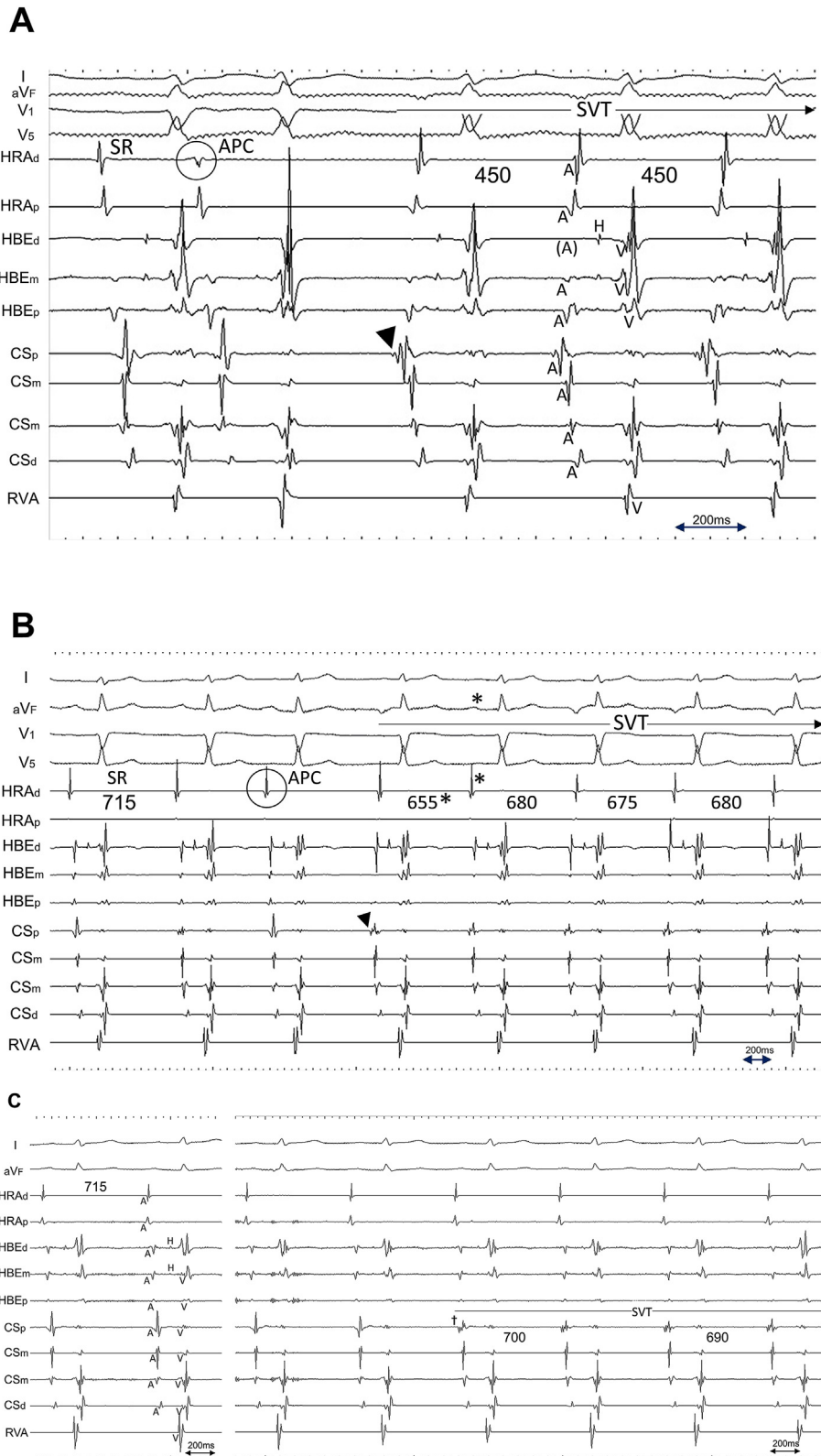


Fig. 2. Intracardiac recordings during SVT induction via premature atrial contraction. Two different types of tachycardia with **A.** short cycle length of 450 ms, and with **B.** long cycle length of 650–700 ms, were induced. A shorter cycle length of 655 ms (asterisk), compared with the following three consecutive beats, is due to the fusion of SVT and premature atrial contraction. Note the earliest atrial activation was consistently observed from the electrodes positioned at the ostium of the coronary sinus (black arrowhead). **C.** Intracardiac recordings (**left**) at rest, and (**right**) during spontaneous SVT induction. Once the electrogram property from the electrodes at the ostium of the coronary sinus (CSp) changed from that of sinus rhythm (dagger), a gradual shortening of atrial cycle length (700 ms–690 ms) and **D.** further shortening of the atrial cycle length (675 ms) consistently surpassed that of sinus rhythm, which consequently provoked the negative P wave morphology at inferior limb lead (aVF). I/aVF, surface ECG leads; CSp/CS_m/CS_d, proximal, mid, and distal coronary sinus electrode, respectively; HBE_d/HBE_m/HBE_p, distal, mid, and proximal electrode of the catheter positioned at the His bundle recording site, respectively; HRA_d/HRA_p, distal and proximal electrode of the catheter positioned at the high lateral right atrium, respectively; RVA, electrode of the catheter positioned at the right ventricular apex; SVT, supraventricular tachycardia.

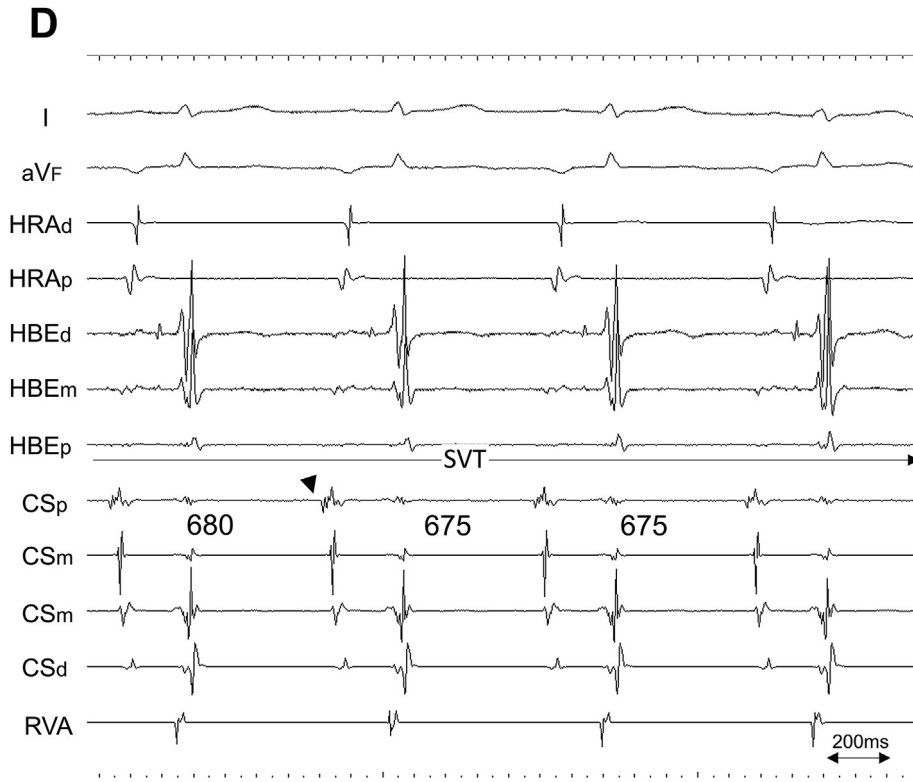


Fig. 2. (continued).

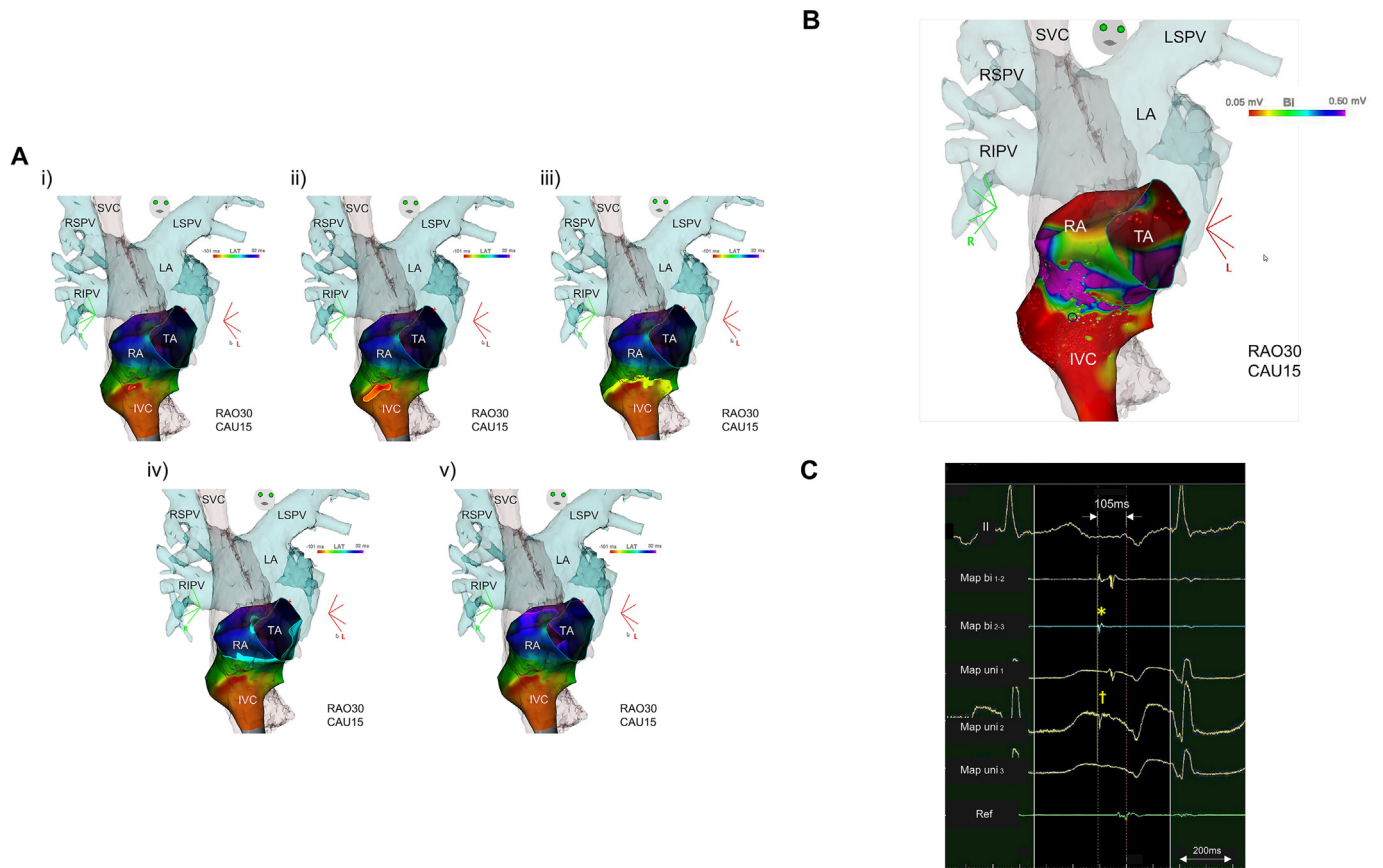


Fig. 3. A. Local activation map and **B.** voltage map, and **C.** intracardiac recordings of atrial tachycardia using a multielectrode mapping catheter. **A., B.:** A centrifugal pattern (i to v) propagating from the EAA (blue circle point) located at the boundary zone between the right atrium and inferior vena cava (red-color code area; <0.05 mV in bipolar voltage map) was observed. **C.:** The potential at the EAA site (asterisk) preceded 105 ms to the P wave onset, QS pattern from the unipolar (dagger), and 0.27 mV from the bipolar electrode, respectively. II, surface ECG leads; CAU, caudal angle; EAA, earliest atrial activation; IVC, inferior vena cava; LA, left atrium; LSPV, left superior pulmonary vein; MAP bi, bipolar electrode from EAA; MAP uni, unipolar electrode from EAA; RAO, right anterior oblique; Ref, reference catheter electrode; RIPV, right inferior pulmonary vein; RSPV, right superior pulmonary vein; SVC, superior vena cava; TA, tricuspid annulus.

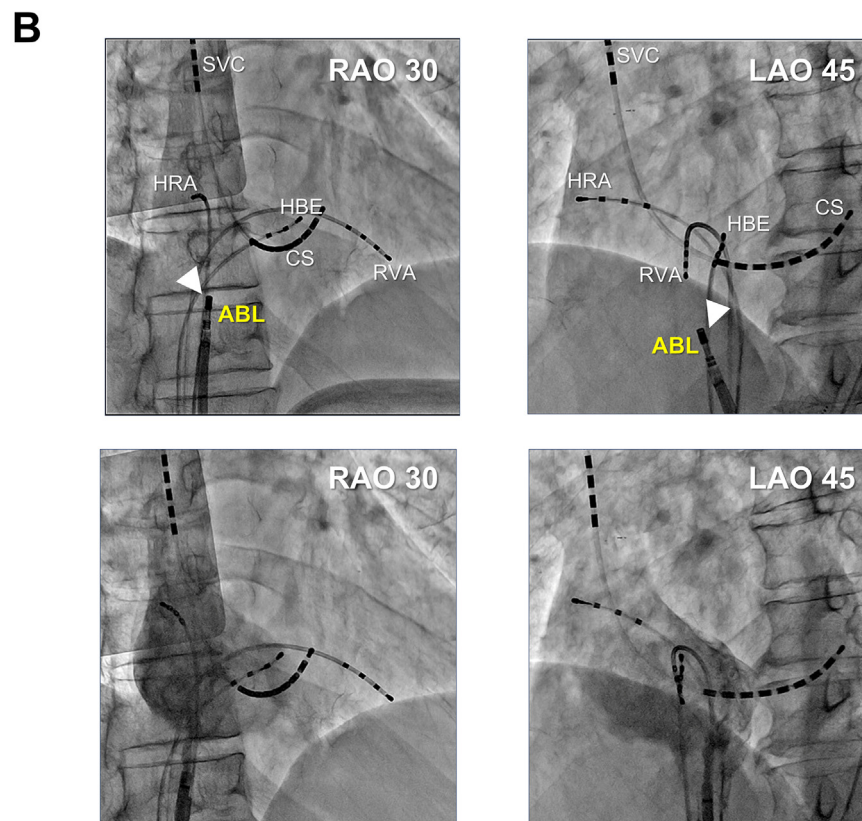
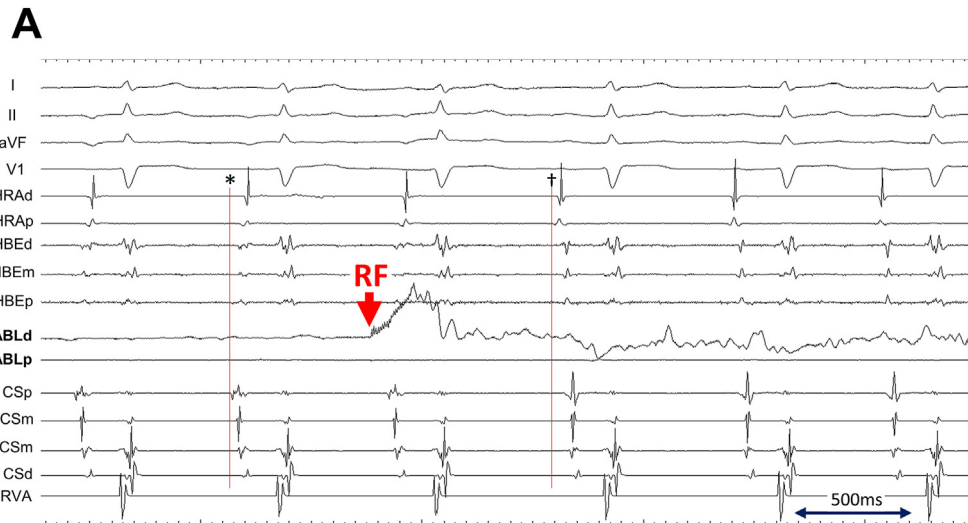


Fig. 4. A. Intracardiac recording and **B.** fluoroscopic image at the successful ablation site. **A.** The distal tip of the ablation catheter was positioned at the earliest atrial activation (EAA) site during AT (cycle length of 695 ms) obtained from a three-dimensional electroanatomical mapping technique using a multielectrode catheter. Based on the abrupt change in atrial potential sequence obtained from each electrode before (asterisk; EAA site was at CSp) and after (dagger; EAA site was at HRAd), the focal radiofrequency energy application site was used for atrial tachycardia termination. Note no distinct potential was observed from the distal tip of the ablation catheter before RF energy application. **B.** Angiography of the right atrium shows the position of the ablation site (white arrow head) just below the right atrium-inferior vena cava junction. I/aVF/V1/V5, surface ECG leads; ABLd/ABLp, distal and proximal electrode of the ablation catheter, respectively; CSp/CSm/CSd, proximal, mid, and distal coronary sinus electrode, respectively; HBEd/HBEm/HBEP, distal, mid, and proximal electrode of the catheter positioned at the His bundle recording site, respectively; HRAd/HRAp, distal and proximal electrode of the catheter positioned at the high lateral right atrium, respectively; LAO, left anterior oblique; RAO, right anterior oblique; SVC, superior vena cava.

catheter (Pentaray) [10]. They demonstrated that although the bipolar voltage amplitude in healthy atria is similar in both electrode catheters (with a fifth percentile of 0.48 and 0.52 mV, respectively), mapping resolution within areas of low voltage and scarring were significantly enhanced with 1-mm multielectrode catheters (1-mm

vs. 3.5-mm; the average of total low voltage area [<0.5 mV]: 14.7 cm² vs. 20.4 cm², $P = 0.02$; and the average of dense scar area [<0.25 mV]: 4.3 cm² vs. 14.2 cm², $P = 0.01$, respectively). As the resolution of 3DEAM is influenced by multiple parameters, including electrode size, interelectrode spacing, angle of incidence

(catheter orientation relative to the surface), the vector of wave propagation and filtering, they therefore concluded that 3DEAM with smaller electrodes and closer interelectrode spacing is more sensitive to detect surviving myocardial fibers in zones where many low voltage channels exist, such as the boundary zone of the thoracic veins and the atrium, as in the present case.

The precise location of the focal source of arrhythmia in the present case may be debatable. As the successful RFCA site was not located deep inside the IVC but at the boundary zone between the RA and IVC according to the angiographic images, any structure around the IVC ostium (i.e., RA myocardial tissue, or part of the ostium of the CS) could be a candidate for the focus. However, the electrophysiological features of a focal source of discharge with or without conduction to the atrium initiating and perpetuating atrial tachyarrhythmia closely resembles those of a PV or CS source and therefore suggest that the origin in the present case was related to a thoracic vein structure.

Funding

None.

References

- [1] Maruyama M, Kobayashi Y, Miyauchi Y, et al. The VA relationship after differential atrial overdrive pacing: a novel tool for the diagnosis of atrial tachycardia in the electrophysiologic laboratory. *J Cardiovasc Electrophysiol* 2007;18(11):1127–33. <https://doi.org/10.1111/j.1540-8167.2007.00928.x>.
- [2] Kistler PM, Roberts-Thomson KC, Haqqani HM, et al. P-wave morphology in focal atrial tachycardia: development of an algorithm to predict the anatomic site of origin. *J Am Coll Cardiol* 2016;48(5):1010–7. <https://doi.org/10.1016/j.jacc.2006.03.058>.
- [3] Huo Y, Braunschweig F, Gaspar T, et al. Diagnosis of atrial tachycardias originating from the lower right atrium: importance of P-wave morphology in the precordial leads V3-V6. *Europace* 2013;15(4):570–7. <https://doi.org/10.1093/europace/eus314>.
- [4] Kistler PM, Fynn SP, Haqqani H, et al. Focal atrial tachycardia from the ostium of the coronary sinus: electrocardiographic and electrophysiological characterization and radiofrequency ablation. *J Am Coll Cardiol* 2005;45(9):1488–93. <https://doi.org/10.1016/j.jacc.2005.01.042>.
- [5] Kistler PM, Sanders P, Fynn SP, et al. Electrophysiological and electrocardiographic characteristics of focal atrial tachycardia originating from the pulmonary veins: acute and long-term outcomes of radiofrequency ablation. *Circulation* 2003;108(16):1968–75. <https://doi.org/10.1161/01.CIR.0000095269.36984.75>.
- [6] Tsai CF, Tai CT, Hsieh MH, et al. Initiation of atrial fibrillation by ectopic beats originating from the superior vena cava: electrophysiological characteristics and results of radiofrequency ablation. *Circulation* 2000;102(1):67–74. <https://doi.org/10.1161/01.cir.102.1.67>.
- [7] Kholová I, Kautzner J. Morphology of atrial myocardial extensions into human caval veins: a postmortem study in patients with and without atrial fibrillation. *Circulation* 2004;110(5):483–8. <https://doi.org/10.1161/01.CIR.0000137117.87589.88>.
- [8] Mansour M, Ruskin J, Keane D. Initiation of atrial fibrillation by ectopic beats originating from the ostium of the inferior vena cava. *J Cardiovasc Electrophysiol* 2002;13(12):1292–5. <https://doi.org/10.1046/j.1540-8167.2002.01292.x>.
- [9] Yamane T, Miyazaki H, Inada K, et al. Focal source of atrial fibrillation arising from the ostium of the inferior vena cava. *Circ J* 2005;69(6):756–9. <https://doi.org/10.1253/circj.69.756>.
- [10] Anter E, Tschabrunn CM, Buxton AE, Josephson ME. High-resolution mapping of postinfarction reentrant ventricular tachycardia: electrophysiological characterization of the circuit. *Circulation* 2016;134(4):314–27. <https://doi.org/10.1161/CIRCULATIONAHA.116.021955>.